文章编号 1004-924X(2012)03-0607-09

超精密机床径推一体式空气静压轴承的静态特性

张飞虎,付鹏强*,汪圣飞,张 强
(哈尔滨工业大学 机电工程学院,黑龙江 哈尔滨 150001)

摘要:提出了一种新的径推一体式静压主轴支撑方式来优化机床主轴系统性能,以满足超精密飞切机床对气体静压轴承高刚度的要求。采用计算流体力学和有限体积法对气体静压轴承气膜内部的流场与压力场进行仿真,并研究其静态特性。为提高计算精度,完成了轴承宏观尺寸与气膜厚度相差几个数量级时气膜厚度方向 2 μm 间距的网格划分。仿真结果表明,在偏心状态下由于气膜压力的变化使节流孔气体流速在 1 ~200 m/s 内变化,机床所采用径推一体式轴承静态刚度达到 3 508 N/μm。研究表明,通过增大轴承的供气压强和减小节流孔的直径可改善轴承的静态性能进而提升机床性能。

关 键 词:空气静压轴承;径推一体轴承;承载力;轴承刚度;超精密机床;计算流体力学
中图分类号:TH133.3;TG502.31 **文献标识码**:A **doi**:10.3788/OPE.20122003.0607

Static characteristics of radial-thrust aerostatic bearing on ultra-precision machine tool

ZHANG Fei-hu, FU Peng-qiang*, WANG Sheng-fei, ZHANG Qiang

(*School of Mechatronics Engineering, Harbin Institute of Technology, Harbin* 150001, *China*)
* *Corresponding author, E-mail: pqfuln@hit.edu.cn*

Abstract: A new vertical spindle supporting system was presented to improve the stiffness of an aerostatic bearing and to meet the requirements of machine tools for aerostatic bearings. The Computational Fluid Dynamics (CFD) and Finite Volume Method (FVM) were used for simulating the flow field and pressure field inside the aerostatic bearing and for researching its static characteristics. The grid subdivision in the direction of film thickness was implemented while establishing the grid of the gas film. Finally, a 2 μm/grid on the thrust surfaces and 2.5 μm/grid on the radial surfaces along the film thickness direction were achieved. Results indicate that the gas velocities around the orifices are about 200 m/s and 1 m/s when the pressure distribution of the gas film is changed and the loading capacity is achieved 3 508 N/μm. It concludes that the static characteristics of the aerostatic bearing can be improved by increasing supply pressures or decreasing the diameters of orifices.

Key words: aerostatic bearing; radial-thrust bearing; loading capacity; bearing stiffness; ultra-precision machine tool; computational fluid dynamics

收稿日期:2012-02-03;**修订日期**:2012-02-08.
基金项目:Supported by National Science and Technology Special Program (No. 2011ZX04004-041); National Natural Science Foundation of China (No. 90923023); Doctoral Program Foundation of Higher Education of China (No. 20092302110055)

1 Introduction

The important advantages of air bearings over conventional bearings are high speed capabilities, high accuracy, low friction, small temperature rises, less pollution and long life[1]. Thus, aerostatic bearings are widely used in precision devices such as precision machine tools, precision measuring equipment and lithography associated production equipment[2-4]. A new kind of radial-thrust aerostatic bearing spindle was designed and used in ultra-precision fly cutting machine tool. A fly cutter head was fixed on the spindle with a large diameter, which can be used to process large optical flat components. This process can be considered as finishing processing and the machined surface can be used directly as optical components without any post-machining such as grinding and polishing[5-6]. So, the manufacturing and working performance of the aerostatic bearing and the spindle will be very good.

The main disadvantages of gas film bearings are their low stiffness, high-speed instability and the high manufacturing precision requirments[7-8]. To improve the performance of the aerostatic bearing, lots of scholars have done a lot of research work. Li and Ding[9] studied on the bearing load capacity and stiffness by using Computational Fluid Dynamics (CFD) method to solve numerically air flow within an orifice and the bearing clearance. They argued that the simulations could predict the experimental load capacity of aerostatic bearings very well. Moreover, Kassab *et al.*[10] indicated that the load capacity and the mass flow rate of a bearing would be increased with the increase of the supply pressure. Schenk *et al.*[11] also pointed out that the stiffness of the orifice-bearing pads increases more rapidly with supplying pressures, and reaches significantly higher values at high supply pressures. Yao *et al.*[12] also analyzed the radial load carrying capacity and stiffness effected by supply pressures and geometrical parameters of gas spherical bearings using Finite Element Method (FEM). They concluded that the static performance of the gas bearing could be improved with the higher supply pressure. Chen and He[13] studied on the relationship between orifice diameter and the performance of the bearing. They indicated that the load capacity would increase with the increase diameter of the orifice under certain supply pressures and film thicknesses. The CFD numerical model was also provided by Lo and Wang[14] to analyze the static performance of a high-precision rotating gas bearing.

Load capacity and stiffness play a key role in the precision and stability of the spindle system. In this paper, the pressure distribution model inside the particular bearing with a radial-thrust coalition structure is simulated based on the CFD software and finite volume method. And then the impact of the gas pressure parameter on the axial performance of the radial-thrust joint bearing is paid more attention. A series of pressure distributions as well as the loading capacity, stiffness and mass flow rate for the bearing with different eccentricity ratios will be revealed.

2 Mathematical model

In this study, the aerostatic bearings model incorporates the following design assumptions:

a) The medium is Newtonian fluid lubrication and laminar flow conditions exist at all points in the gas film.

b) Gas lubricating films are very nearly isothermal because the ability of the bearing materials to conduct away heat is greater than the heat generating capacity of the gas film. Thus, we may assume that the flow is isothermal.

c) The mass flow inside and outside of the gas bearing element is equal to the mass flow into the orifice.

d) Inertia forces due to acceleration can be

neglected compared to frictional forces due to viscous shearing and there is no slip at the boundaries between the fluid and the thrust plates.

The pressure distribution in the gas film between the shaft and the bushing is modeled by the Reynolds equation base on the assumptions above as follows:

$$\frac{\partial}{\partial x}\left(h^3 p \frac{\partial p}{\partial x}\right)+\frac{\partial}{\partial y}\left(h^3 p \frac{\partial p}{\partial y}\right)= 6\left[\frac{\partial}{\partial x}ph(u_1+u_2)+\frac{\partial}{\partial y}ph(v_1+v_2)\right], \quad (1)$$

The dimensionless form of the Reynolds equation in order to simplify the calculation is given by:

$$\frac{\partial}{\partial \bar{x}}\left(\bar{h}^3 \frac{\partial \bar{p}^2}{\partial \bar{x}}\right)+\frac{\partial}{\partial \bar{y}}\left(\bar{h}^3 \frac{\partial \bar{p}^2}{\partial \bar{y}}\right)+\bar{Q}\delta_i= \Lambda_x \frac{\partial(\bar{h}\bar{p})}{\partial \bar{x}}+\Lambda_y \frac{\partial(\bar{h}\bar{p})}{\partial \bar{y}}, \quad (2)$$

where Λ_x and Λ_y are the bearing numbers in the x- and z-directions, respectively, and $\bar{Q}$ is the mass flow factor of the orifice. It is noted that Kronecker symbol $\delta_i=1$ at the orifice entrance, and that $\delta_i=0$ at the orifice exit.

The following dimensionless parameters are defined:

$$p=p_0\bar{p},\ h=h_m\bar{h},\ x=l\bar{x},\ y=l\bar{y},\ t=\frac{l}{V}\bar{t},$$

$$\Lambda_x=\frac{12\eta u l}{h_m^2 p_0},\ \Lambda_y=\frac{12\eta v l}{h_m^2 p_0},\ \bar{Q}=\frac{24\eta l^2 p_a}{h_m^3 p_0^2 \rho_a}\rho \tilde{v}.$$

When the pressure distribution p is known, the bearing performance can be determined. The bearing axial load capacity W can be obtained by the integral transform of the gas film pressure on the upper and lower thrust bearing surfaces respectively, shows as below:

$$W=\iint_{A_{up}} p_{up}\,dx\,dy-\iint_{A_{lower}} p_{lower}\,dx\,dy. \quad (3)$$

The bearing stiffness K is derived from the variation of the bearing load capacity as a function of the film thickness,

$$K=-\frac{\Delta W}{\Delta h}. \quad (4)$$

Adopting the assumptions above, it can be shown that the mass flow rate is given by:

$$\dot{m}_{Ar}=\pi d_0 h p_0 \varphi\sqrt{\frac{2\rho_0}{p_0}}\cdot\Psi_g, \quad (5)$$

$$\Psi_g=\begin{cases}\left[\frac{k}{2}\left(\frac{2}{k+1}\right)^{\frac{(k+1)}{(k-1)}}\right]^{\frac{1}{2}}, & \frac{p}{p_0}\leqslant\beta_k \\ \left\{\frac{k}{k-1}\left[\left(\frac{p}{p_0}\right)^{\frac{2}{k}}-\left(\frac{p}{p_0}\right)^{\frac{(k+1)}{k}}\right]\right\}^{\frac{1}{2}}, & \frac{p}{p_0}>\beta_k\end{cases},$$

where φ is the coefficient of the mass flow rate through the orifice, k is the ratio of the specific heat, p_0 is the supplied pressure, and $\beta_k=p_c/p_0$.

3 Structure of the radial-thrust joint bearing

The ultra-precision fly cutting machine for cutting large diameter optical components was designed in vertical structure as shown in Fig. 1. The diagrammatic sketch of the aerostatic bearing used on the machine tool is shown in Fig. 2. The whole bearing system is composed of two thrust bearings and one radial bearing which has the public atmospheric boundary at the two junctions of the bearing. There are 18 uniform orifices in each end of the spindle sleeve and each of the double rows along the radial bearing. The

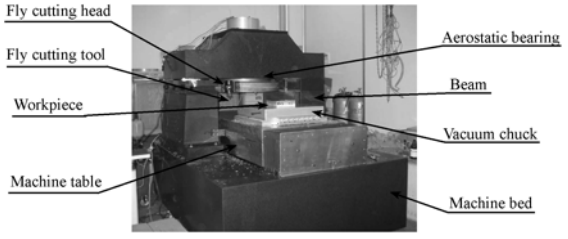

Fig. 1　Structure schemes of the ultra-precision fly cutting machine

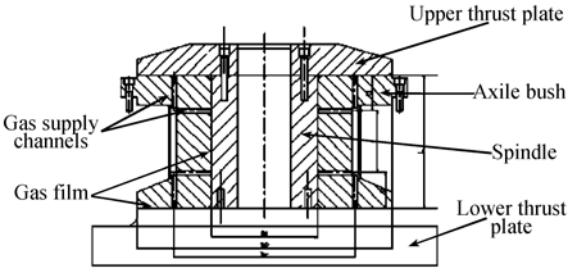

Fig. 2　Schematic diagram of aerostatic bearing structure

air film is an annulus with an inner diameter of $D_1 = 220$ mm and an outer diameter of $D_2 = 440$ mm. The single side clearance of the air film in the radial bearing is $h_1 = 0.015$ mm and in the thrust bearing is $h_2 = 0.012$ mm. All of the orifices' diameters are $d = 0.2$ mm.

4 Numerical solution method

Before using the CFD software to solve the problem, the first step is to establish bearing film structural model using gambit pre-processing software. This paper studies on the thrust bearing lubrication performance. Therefore, the main related factor is the changes of the gas film thickness on the surfaces of the upper and lower thrust bearing. In this case, in order to simplify the calculation, the whole film is divided into six equal portions since the bearing symmetry in the circumferential direction, and just the 1/6 is taken as the study objective, shown as Fig. 3. This strategy can greatly reduce the number of film grids and improve the computational efficiency.

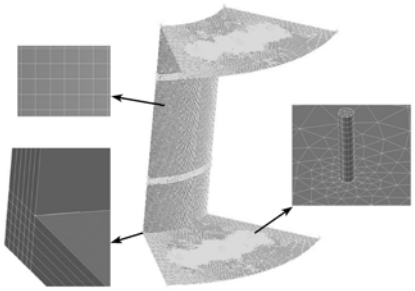

Fig. 3　Meshing of gas film

It is not difficulty to establish the mesh structure for the size with the magnitude equivalent to every direction of fluid flow. In this study, it is also easy to do if ignoring the gas film thickness, and the gas film structure as a surface element. However, they do not reflect the pressure variation in the film thickness direction and expense the computational accuracy. In this paper, the pressure changes and grid subdivision in the direction of film thickness are paying more attentions when established the grid of the whole gas film. A number of difficulties should be solved due to this specific bearing structure and the higher request of the grid. a) Compared with thickness direction of the film, the other two directions are too large that meshed grid distortion is often emerged; b) It is more complex of the specific film structure near the orifice; c) There is special mutations case of the film thickness at the junction of thrust part and radial part. In addition, the greater the number of the grids is, the more accurate results can be obtained theoretically. Moreover, in the same time, the calculation time will be longer and the requirements of the computer's hardware will be higher.

To solve the problems above, to meshing the bearing film respectively is needed for each piece of mesh. The meshing of the gas film is shown as Fig. 3. a) The grid nodes of the orifice circumferential direction are eight. b) Along the direction of the film thickness, the numbers of the nodes both are six in the radial and thrust surfaces. That is, 2 μm/grid on the thrust surfaces, and 2.5 μm/grid along film thickness direction on the radial surface. c) In other dimension direction, The interval size is set to 2, that is, there is a node every 2 mm. For the shape of the grids, near the orifice used in the prism grid, the other parts are hexahedral mesh.

5 Static bearing characteristics

5.1 Pressure and flow velocity distribution

It is very difficult to give the precise analytical pressure distribution, as the actual gas flow in the aerostatic bearing gap is a complex three-dimensional flow. The CFD software can give relatively accurate details of the fluid flow, such as the time-varying characteristics distribution of velocity, pressure, density, temperature and so on[15-16]. Thus, the software not only can predict

the overall performance of the air film and can easily find the bearing problems in design or engineering from the analysis[17-18]. The results can describe the gas bearing lubrication characteristics with the lubrication equation above.

The distribution of the gas film pressure of the joint bearing is shown in Fig. 4. The pressure distribution when the axial offset $e = 0$ μm is shown as Fig. 4 (a). The gas film thicknesses of the upper and lower thrust surfaces both are 12 μm. The pressure distribution is almost consistent between these two surfaces. Fig. 4 (b) is for the e=7 μm. The pressure on the upper surface was significantly greater than that on the surface below since the upper one is for a small air gap and the lower one is for a large gap.

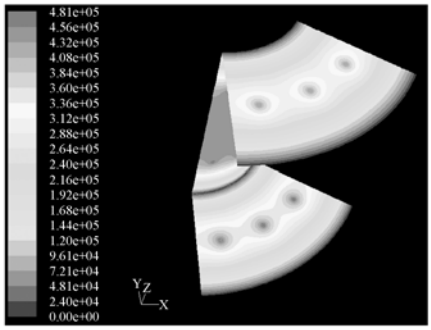

(a) $e = 0$ μm

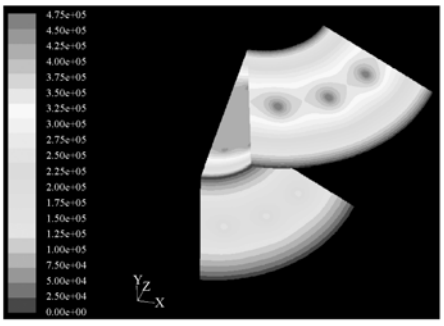

(b) $e = 7$ μm

Fig. 4　Distribution image of gas film pressure

Fig. 5 is the velocity field of the gas film under the condition that the supply pressure $p_s = 0.5$ MPa, orifice diameter $d_c = 0.2$ mm, and orifice holes $n = 18$, the bearing axial offset $e = 7$ μm. According to Fig. 4 (b), the pressure of the upper thrust surface is high while the pressure on the lower surface is small. When the supply pressure is constant, the airflow speed is small on the upper surface of the bearing and the that is great on the lower one. This velocity distribution is agreed with the situation in Fig. 5. We can see that the gas velocity around the lower orifice is about 200 m/s, while that around the upper orifice is less than 1 m/s. This velocity difference is caused by the different pressure distribution between them, as shown in Fig. 4 (b).

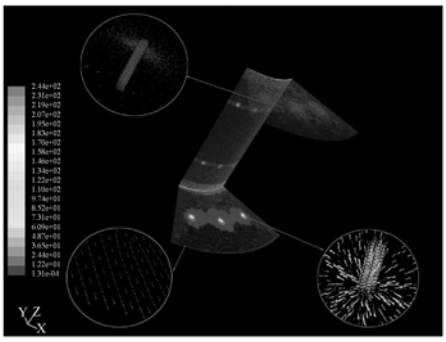

Fig. 5　Velocity field of the gas film

5.2　Static characteristics

The static characteristics of this special bearing using on the ultra-precision fly cutting machine can be obtained from the numeric model. With the parameters mentioned above, when the supply pressure is 0.5 MPa, and the axial offset is 1 μm, the calculation of the loading capacity and the mass flow rate are respectively 3 508 N and 11.94×10^{-4} kg/s. According to formula (4) the static stiffness of the bearing is 3 508 N/μm.

The present study investigates the effects of gas supply pressure, orifice diameter and offset upon the loading capacity, stiffness and mass flow rate change of a radial-thrust coalition structure bearing. The gas supply pressure is 0.3, 0.4, 0.5, 0.6 and 0.7 MPa. The machine spindle axis offset changes from 0 μm to 7 μm every 1 μm. The orifice diameter values are 0.1, 0.2 and 0.3 mm. The carrying capacity, stiff-

ness and the gas mass flow of the bearing are calculated to find the continuity and regularity of these parameters changed. The results are shown in Figs. 6～11.

From Figs. 6～8, it is observed that as the supply pressure increases, the axial load capacity and stiffness characteristics are increased approximately while the mass flow rate increased increasingly. The axial load capacity is increased significantly with the increase of the axial offset and showed a clear linear law when the supply pressure is constant. The axial stiffness tends to decrease with the axial offset increases and it is evident with the large gas pressure. The mass flow rate and axial offset of the bearing have a little relationship from Fig. 8. It is decrease with the offset value while the supply pressure is more than 0.4 MPa and slight increase while the pressure is 0.3 MPa. Overall, increased the supply pressure can significantly improve the axial load bearing capacity and the bearing stiffness, but also make the gas mass flow increases.

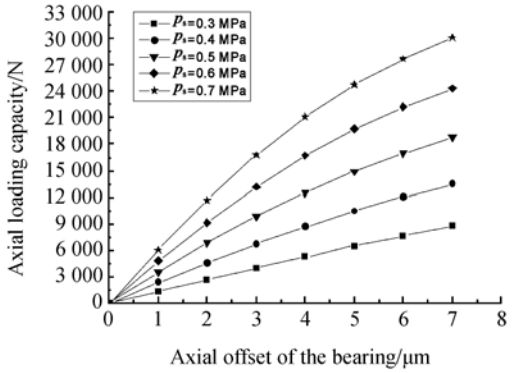

Fig. 6 Axial loading capacity of gas film with offset values under different supplied pressures

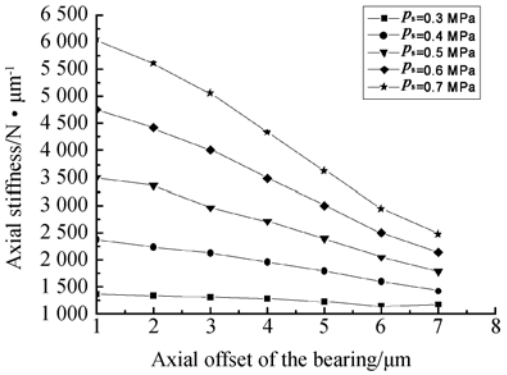

Fig. 7 Axial stiffness of a gas bearing changes with offset values under different supplied pressures

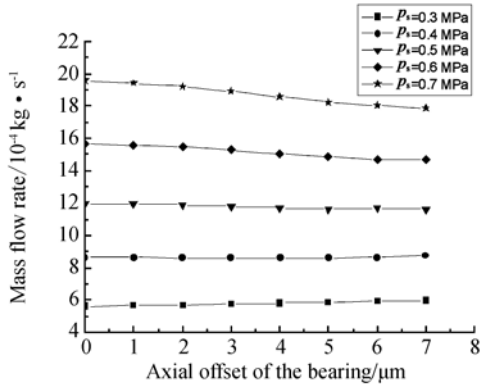

Fig. 8 Mass flow rate of a gas bearing changes with offset values under different supplied pressures

From Fig. 9, the bearing load capacity is increase with the axial offset increases when the orifice diameter is a certain value. The carrying capacity is significantly reduced with the increase diameter of the orifice diameter when the axial offset is constant. Fig. 10 indicates that the bearing axial stiffness increases with the decreases of the orifice diameter. However, the performance is different when the offset increase. When the orifice diameter is small, the bearing stiffness will significantly reduced with the increase of the axial offset, and in larger orifice diameter, for 0.3 mm, the impact of the bearing offset on the bearing stiffness is not obvious.

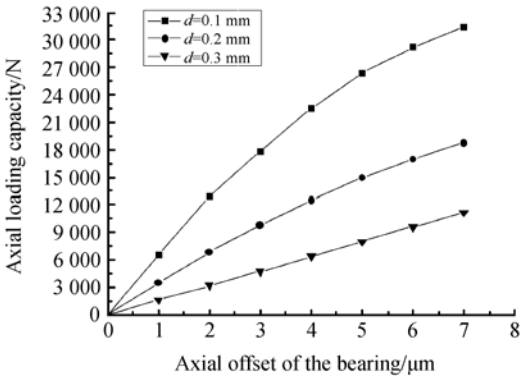

Fig. 9 Axial loading capacity of gas film with offset values under different orifice diameters

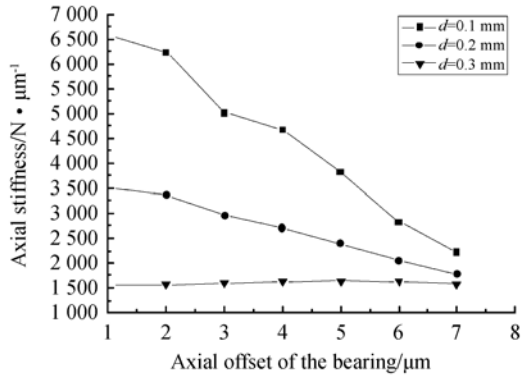

Fig. 10　Axial stiffness of a gas bearing changes with offset values under different orifice diameters

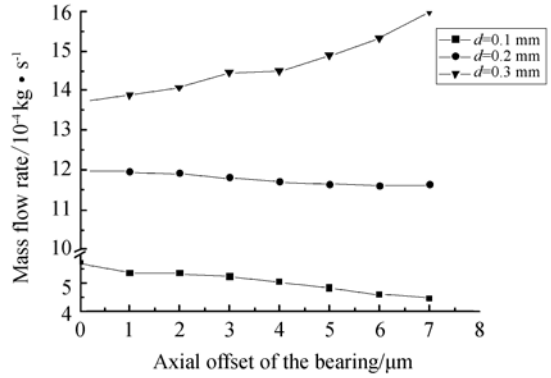

Fig. 11　Mass flow rate of a gas bearing changes with offset values under different orifice diameters

Fig. 11 shows that the consumption of the supply gas will increase as the increased orifice diameter. The conclusion maybe like this: to improve the static performance of the bearing, increasing the load capacity and axial stiffness and reducing the air consumption, should reduce the orifice diameter. In fact, it can be seen that from these figures, when the orifice diameter is 0.1 mm, the bearing performance has shown the unsteadiness which indicating that in this case, it is easy to induce the spindle instability once the random external force acting on the bearing. From the view of the engineering point, it is easy to lead to blocking for smaller diameter holes that affect the bearing performance. For the same time, it is greater difficulty to process the small holes and the scale errors acting on the performance can not be ignored, the error consistency is difficult to guarantee.

6　Conclusions

This study has investigated the performance of radial-thrust joint aerostatic bearings using the ultra-precision fly cutting machine spindle and the effects of the gas supply pressure, orifice diameter and offset upon the load capacity, stiffness and mass flow rate. From the numerical simulation results and associated discussion above, the following conclusions can be drawn:

a) Compared with thickness direction of the film, the other two directions are too large that meshed grid distortion is often emerged. The meshing along the direction of the gas film thickness has been achieved with 2 μm space.

b) The radial-thrust joint aerostatic bearings developed can supply high load capacity and stiffness, which can achieve 3 508 N/ μm. In addition, the values of them increase as the supply pressure increases.

c) For a certain value of the supply pressure, as the supply orifice diameter increases, the load capacity and stiffness decrease while the mass flow rate increases.

7　Acknowledgements

This work was supported by the National Science and Technology Special Program "High-end CNC machine tools and basic manufacturing equipment" (No. 2011ZX04004-041), the National Natural Science Foundation of China (No. 90923023) and the Doctoral Program Foundation of Higher Education of China, No. 20092302110055.

参考文献：

[1] AN CH H, ZHANG Y, XU Q, *et al.*. Modeling of dynamic characteristic of the aerostatic bearing spindle in an ultra-precision fly cutting machine [J]. *International Journal of Machine Tool & Manufacture*, 2010, 50: 374-385.

[2] YE SH L, LI D SH. Study on mechanical characteristics of aerostatic bearing with finite volume method [J]. *Opt. Precision Eng.*, 2008, 16(5): 809-814. (in Chinese)

[3] MIYATAKE M, YOSHIMOTO S. Numerical investigation of static and dynamic characteristics of aerostatic thrust bearings with small feed holes [J]. *Tribology International*, 2010, 43: 1353-1359.

[4] ZHANG J H, ZHANG SH G, ZHAO H X, *et al.*. Structure design and test for guide unloading system of large ultraprecision machine [J]. *Opt. Precision Eng.*, 2007, 15(9): 1382-1390. (in Chinese)

[5] LEE W B, CHEUNG C F. A dynamic surface profile model for the prediction of nano surface generation in ultra-precision machining [J]. *International Journal of Mechanical Sciences*, 2001, 43: 961-991.

[6] ZHAO Q L, GUO B, YANG H, *et al.*. Technological parameter optimization of micro-structured surfaces by diamond fly-cutting [J]. *Opt. Precision Eng.*, 2009, 17(10): 2512-2519. (in Chinese)

[7] FREW D A, SCHEFFER C. Numerical modelling of a high-speed rigid rotor in a single-aerostatic bearing using modified Euler equations of motion [J]. *Mechanical Systems and Signal Processing*, 2008, 22: 133-154.

[8] LIU Q, ZHANG C P. H-type air bearing motion stage driven by linear motors [J]. *Opt. Precision Eng.*, 2007, 15(10): 1540-1546. (in Chinese)

[9] LI Y T, HAN D. Influences of the geometrical parameters of aerostatic thrust bearing with pocketed orifice-type restrictor on its performance [J]. *Tribology International*, 2007, 40: 1120-1126.

[10] KASSAB S Z, NOUELDEEN E M, SHAWKY M A. Effects of operating conditions and supply hole diameter on the performance of a rectangular aerostatic bearing [J]. *Tribology International*, 1997, 30: 533-545.

[11] SCHENK C, BUSCHMANN S, RISSE S, *et al.*. Comparison between flat aerostatic gas-bearing pads with orifice and porous feedings at high-vacuum conditions [J]. *Precision Engineering*, 2008, 32: 319-328.

[12] YAO Y X, QIN D L, ZHANG H B. Static performance analysis of orifice compensated externally pressurized gas spherical bearing based on FEM [J]. *Key Engineering Materials*, 2006, 315-316: 860-863.

[13] CHEN X D, HE X M. The effect of the recess shape on performance analysis of the gas-lubricated bearing in optical lithography [J]. *Tribology International*, 2006, 39: 1336-1341.

[14] LO CH Y, WANG CH CH, LEE Y H. Performance analysis of high-speed spindle aerostatic bearings [J]. *Tribology International*, 2005, 38: 5-14.

[15] JI S M, MA B L, TAN D P. Numerical analysis of soft abrasive flow in structured restraint flow passage [J]. *Opt. Precision Eng.*, 2011, 19(9): 2092-2099. (in Chinese)

[16] LIU X J, CHEN R W. Finite element analysis and experiments on Rainbow shape piezoelectric energy transferring elements [J]. *Opt. Precision Eng.*, 2011, 19(4): 789-796. (in Chinese)

[17] KHATAIT J, LIN W, LIN W J. Design and development of orifice-type aerostatic thrust bearing [J]. *SIMTech technical reports*, 2005, 6(1): 7-12.

[18] WANG Z, LI Z H. Design of optical-mechanical structure for lunar-based extreme ultraviolet camera [J]. *Opt. Precision Eng.*, 2011, 19(10): 2427-2433. (in Chinese)

Authors' biographies:

ZHANG Fei-hu (1964 —), male, was born in Henan province. He received his MS and BS from Northwestern Polytechnical University in 1987 and 1984 respectively and PhD degree from Harbin Institute of Technology in 1993. Now He is a Professor of Mechanical Engineering at the School of Mechatronics Engineering of Harbin Institute of Technology. His research interests include new methods and technology of ultra-precision machining and equipment like ultra-precision ELID grinding technology, ultra-smooth surface magnetorheological finishing technology and ultra-precision fly cutting machine tool. E-mail: zhangfh@hit.edu.cn

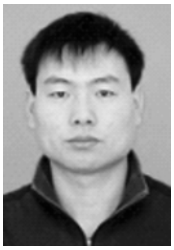

FU Peng-qiang (1983 —), male, He was born in Shanxi province and received his BS and MS degrees from Harbin Institute of Technology. Now he is a Ph. D student of mechanical engineering at the School of Mechatronics Engineering of Harbin Institute of Technology. He has extensive research interests in manufacturing technology of ultra-precision machining equipment and the related study on the spindle of the machine tool. E-mail: pqfuln@hit.edu.cn

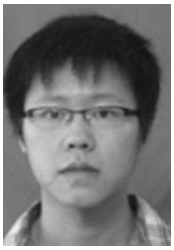

Wang Sheng-fei (1985 —), male, Ph. D student. He was born in Sichuan province and received his BS and MS degrees in School of Mechatronics Engineering from Harbin Institute of Technology. His current research interests include aerostatic bearing and numerical simulation. Email: robertwsf@sina.com

ZHANG Qiang (1985 —), male, mechanical engineer. He was born in Heilongjiang province and obtained his BS degree in mechanical engineering from Jiamusi University. He is working on the manufacturing technology of the ultra-precision machining equipment, design and manufacturing of the non-standard equipment and ultra-precision processing technology. E-mail: qiangzi0814@163.com